# A general locomotion control framework for multi-legged locomotors

Baxi Chong[1*], Yasemin O. Aydin[1*], Jennifer M. Rieser[2], Guillaume Sartoretti[3],
Tianyu Wang[1], Julian Whitman[4], Abdul Kaba[5], Enes Aydin[1], Ciera McFarland[6],
Kelimar Diaz Cruz[1], Jeffery W. Rankin[7], Krijn B Michel[8], Alfredo Nicieza[9],
John R Hutchinson[8], Howie Choset[4] and Daniel I. Goldman[1]

[1] School of Physics, Georgia Institute of Technology

[2] Physics Department, Emory University

[3] Department of Mechanical Engineering, National University of Singapore

[4] Robotics Institute, Carnegie Mellon University

[5] Morehouse College

[6] Pennsylvania State University

[7] Rancho Research Institute

[8] Royal Veterinary College

[9] University of Oviedo

[*] Corresponding author. Email: daniel.goldman@physics.gatech.edu [+] Equally contributed.

## Text

### Numerical Derivation of Local Connection Matrix

#### Force and torque balance in the vertical plane

In Eq. 2, we prescribed the contact pattern by its phase, $\phi_1$. However, the supporting force (against gravity) is not uniformly distributed among all the legs in stance phase, especially when the robot locomote on the flat hard ground. In order to precisely model the friction, we need to calculate the supporting force distribution among legs.

As shown in Fig. S2, we labeled the legs in stance phase with numbers. The location of

1

each leg is represented as $[x_i\ y_i]$ with respect to a pre-chosen coordinate. The supporting force on each leg is $N_i$. Assuming that all the legs are elastic bodies, the supporting force on each leg can be calculated as:

$$N_i = \begin{cases} KL\epsilon_i, & \text{if } K\epsilon_i \leq 0 \\ 0, & \text{otherwise} \end{cases} \tag{S.1}$$

where $\epsilon_i$ is the strain at leg $i$ in stance phase; K is the spring constant and L is the leg length. As suggested in [6], it is reasonable to assume that the robot is a toppling table. In other words, we assume that only the legs are deformable bodies whereas the deformation in the ground substrate and in the main robot body is negligible. In this way, the distance of the body plane and the ground plane at location $[x_i\ y_i]$ in a fixed reference coordinate can be expressed as:

$$L_i = [x_i\ y_i\ 1] \begin{bmatrix} e_1 \\ e_2 \\ d \end{bmatrix} \tag{S.2}$$

where $e_1$ and $e_2$ are tilt angle in x and y direction and $d$ is the constant offset. Note that the distance of body plane and the ground plane can relate to the strain as:

$$\epsilon_i = (L_i - L)/L = [x_i\ y_i\ 1] \begin{bmatrix} e_1/L \\ e_2/L \\ (d-L)/L \end{bmatrix} = [x_i\ y_i\ 1] \begin{bmatrix} e_1' \\ e_2' \\ d' \end{bmatrix}. \tag{S.3}$$

Therefore, the collection of the supporting forces of all legs is:

$$\boldsymbol{\epsilon} = \begin{bmatrix} \epsilon_1 \\ \epsilon_2 \\ \dots \\ \epsilon_n \end{bmatrix} = \begin{bmatrix} x_1 & y_1 & 1 \\ x_2 & y_2 & 1 \\ \dots & \dots & \dots \\ x_n & y_n & 1 \end{bmatrix} \begin{bmatrix} e_1' \\ e_2' \\ d' \end{bmatrix}, \tag{S.4}$$

for simplicity of notation, we define:

$$S = \begin{bmatrix} x_1 & y_1 & 1 \\ x_2 & y_2 & 1 \\ \dots & \dots & \dots \\ x_n & y_n & 1 \end{bmatrix}, \boldsymbol{\epsilon} = S \begin{bmatrix} e_1' \\ e_2' \\ d' \end{bmatrix}.$$

2

Next, the force and torque balance in the vertical plane can be written as:

$$\begin{bmatrix} x_c \\ y_c \\ 1 \end{bmatrix} mg = \begin{bmatrix} x_1 & x_2 & ... & x_n \\ y_1 & y_2 & ... & y_n \\ 1 & 1 & ... & 1 \end{bmatrix} \begin{bmatrix} N_1 \\ N_2 \\ ... \\ N_n \end{bmatrix}, \tag{S.5}$$

where $[x_c \ y_c]$ is the coordinate of the center of mass. With Eq. (S1-S5), we can numerically calculate the supporting force distribution on legs in stance phase $\boldsymbol{N}$. Note that in the simple linear case,

$$\boldsymbol{N} = -S(S^T S)^{-1} \begin{bmatrix} x_c \\ y_c \\ 1 \end{bmatrix} mg, \tag{S.6}$$

is the solution to Eq. (S1-S4), if the obtained $\boldsymbol{N} < 0$ (element-wise).

**Force and torque balance in the lateral plane**

In this section, we will briefly describe the steps to numerically calculate the local connection matrix. We refer readers to [2, 8] for detailed derivation.

The ground reaction force (GRF) experienced by the robot is the sum of the GRF experienced by each body segment in stance phase, as show in example in Fig. S3. In each body segments in contact with substrate ($c_i = 1$), the GRF, $f_i$, is directed related to its body velocity ($\xi_i$) (see Fig. S3). In the isotropic environments, the direction of $f_i$ is solely determined by the direction of $\xi_i$. For example, in the isotropic Coulomb friction model, the GFR can be related to the body velocity by:

$$f_i = \mu N_i \frac{\xi_i}{|\xi_i|} \tag{S.7}$$

where $\mu$ is the friction coefficient and $N_i$ is its supporting force.

In the anisotropic environments, the direction of GFR is also related to the orientation of the limb. Specifically, we choose x axis to be along the direction parallel to the limb orientation,

and y axis to be perpendicular to the direction of the limb orientation. We then decompose $f_i$
and $\xi_i$ into x and y directions as:

$$f_i = \begin{bmatrix} f_x^i & 0 \\ 0 & f_y^i \end{bmatrix} \begin{bmatrix} \hat{x} \\ \hat{y} \end{bmatrix}, \xi_i = \begin{bmatrix} \xi_x^i & 0 \\ 0 & \xi_y^i \end{bmatrix} \begin{bmatrix} \hat{x} \\ \hat{y} \end{bmatrix}. \tag{S.8}$$

We showed examples of such decomposition in Fig. S3. In the anisotropic Coulomb friction
model [7, 5], the x, y component of the GRF and the body velocity can be related as:

$$\begin{bmatrix} f_x^i \\ f_y^i \end{bmatrix} = \frac{N_i}{|\xi_i|} \begin{bmatrix} \mu_x & 0 \\ 0 & \mu_y \end{bmatrix} \begin{bmatrix} \xi_x^i \\ \xi_y^i \end{bmatrix} \tag{S.9}$$

In the poppy seed RFT model [3], the x, y component of the GRF and the body velocity can
be related as:

$$f_y = C \sin(\gamma) \tag{S.10}$$

$$f_x = A \cos(\gamma) + B(1 - \sin(\gamma)) + F_0 \tag{S.11}$$

where $\gamma = \arctan(\xi_y/\xi_x)$; $C = 0.66$, $A = 0.27$, $B = -0.32$, $F_0 = 0.09$ is the emporical fitted
function to characterize the granular media resistant force.

Note that in each configuration, the body velocity of the body segment $i$, $\xi_i$, can be related
to the body velocity of the locomotor (in our case, we choose head frame as the body frame of
the locomotor) $\xi_0$, by [1, 4]:

$$\xi_i = \text{Ad}_{g_{0i}^{-1}} \xi_0 + J_i(\mathbf{\Phi}) \dot{\mathbf{\Phi}} \tag{S.12}$$

where $J_i(\mathbf{\Phi}) \in \mathbb{R}^{3 \times 3}$ is the body Jacobian matrix, a linear differential map from shape velocity
$\dot{\mathbf{\Phi}}$ to the body velocity of body segment $i$ with respect to the head frame; $\text{Ad}_g$ denotes the adjoint
operator, which maps body velocity between different frames; $g_{0l}$ denotes the configuration of

the body frame of body segment i with respect to the head frame. Note that $\text{Ad}_{g_{0i}^{-1}}$ and $J_i(\boldsymbol{\Phi})$ are uniquely determined by the shape variable $\boldsymbol{\Phi}$.

Finally, the force and torque balance in the lateral plane can be written as:

$$\sum_{i=1}^{n} f_i^0 = \sum_{i=1}^{n} \text{Ad}_{g_{0i}^{-1}}^{T} \begin{bmatrix} f_x^i \\ f_y^i \\ 0 \end{bmatrix} = 0 \tag{S.13}$$

where $f_i^0$ denoted the force applied to body segment $i$ with respect to the head frame; $\text{Ad}_{g_{0i}^{-1}}^{T}$ transforms the force in the body frame to the head frame.

With Eq. (S7-S13), we established a relationship between the body velocity in the head frame $\xi_0$ and the shape velocity $\dot{\boldsymbol{\Phi}}$ and shape velocity $\boldsymbol{\Phi}$. We then linearilize the equations then we can obtain:

$$\xi_0 = A(\boldsymbol{\Phi})\dot{\boldsymbol{\Phi}}. \tag{S.14}$$

# References

[1] Chaohui Gong, Daniel I Goldman, and Howie Choset. Simplifying gait design via shape basis optimization. In *Robotics: Science and Systems*, 2016.

[2] Ross L Hatton, Yang Ding, Howie Choset, and Daniel I Goldman. Geometric visualization of self-propulsion in a complex medium. *Physical review letters*, 110(7):078101, 2013.

[3] Benjamin McInroe, Henry C Astley, Chaohui Gong, Sandy M Kawano, Perrin E Schiebel, Jennifer M Rieser, Howie Choset, Richard W Blob, and Daniel I Goldman. Tail use improves performance on soft substrates in models of early vertebrate land locomotors. *Science*, 353(6295):154–158, 2016.

[4] Richard M Murray, Zexiang Li, S Shankar Sastry, and S Shankara Sastry. *A mathematical introduction to robotic manipulation*. CRC press, 1994.

[5] Aksel A Transeth, Remco I Leine, Christoph Glocker, and Kristin Y Pettersen. 3-d snake robot motion: nonsmooth modeling, simulations, and experiments. *IEEE transactions on robotics*, 24(2):361–376, 2008.

[6] James R Usherwood and Benjamin JH Smith. The grazing gait, and implications of toppling table geometry for primate footfall sequences. *Biology letters*, 14(5):20180137, 2018.

[7] SV Walker and RI Leine. Set-valued anisotropic dry friction laws: formulation, experimental verification and instability phenomenon. *Nonlinear Dynamics*, 96(2):885–920, 2019.

[8] Baxi Zhong, Yasemin Ozkan Aydin, Chaohui Gong, Guillaume Sartoretti, Yunjin Wu, Jennifer Rieser, Haosen Xing, Jeffery Rankin, Krijn Michel, Alfredo Nicieza, et al. Coordination of back bending and leg movements for quadrupedal locomotion. In *Robotics: Science and Systems*, 2018.

# Supplement Figures

a. Quadrupeds
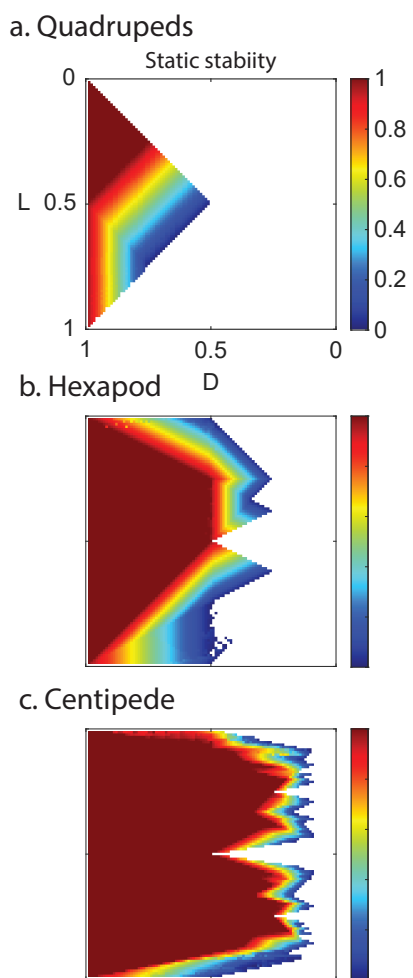


b. Hexapod



c. Centipede



Figure S1: **Static stability for gaits with body undulation** Theoretical predicted static stability of gaits with properly coordinated body undulation for (a) quadrupeds (b) hexapod, and (c) myriapods. All the panels have the same axis as in (a).
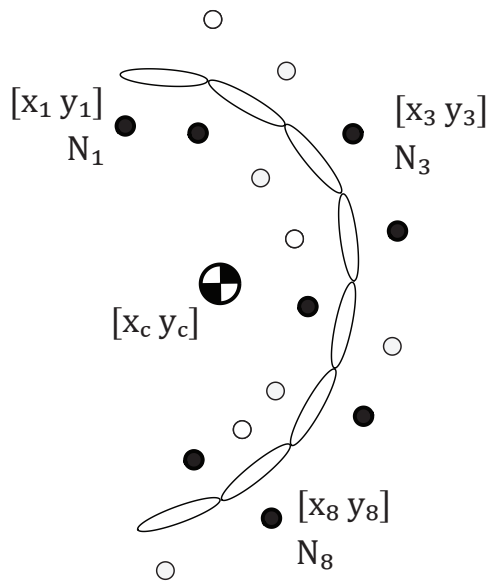
Figure S2: **Supporting force distribution** An example of myriapod model. In this example, the robot is supported by eight legs. For a leg i, it provides supporting force $N_i$. Its location is labeled as $[x_i \ y_i]$. The location of center of mass is labeled $[x_c \ y_c]$
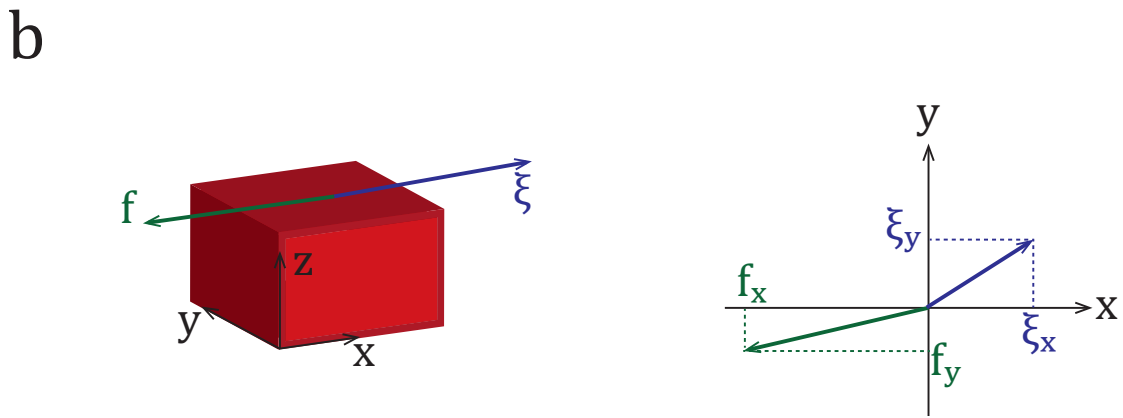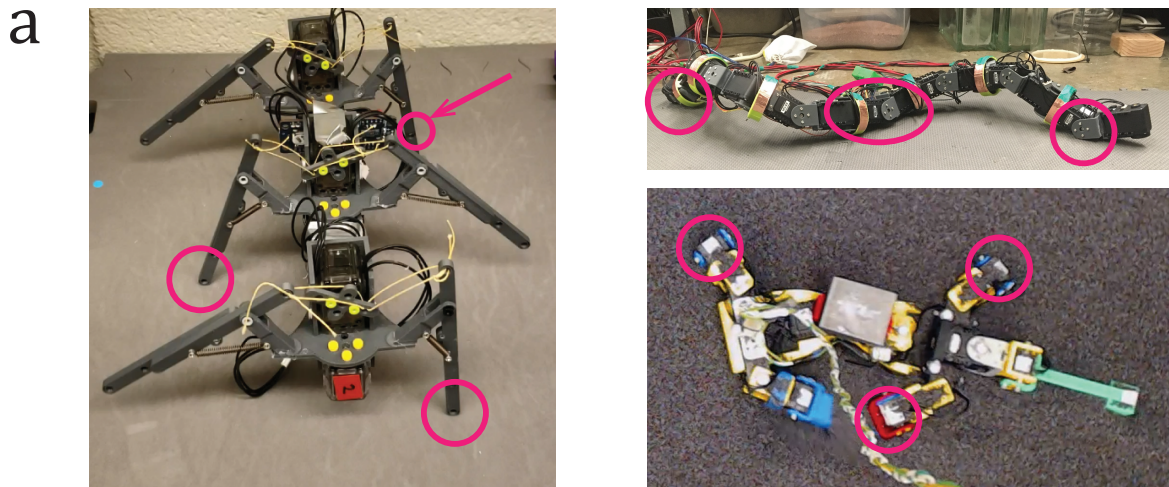
Figure S3: **Relationship between the body velocity and ground reaction force** (a) The robots with hybrid contact with environments. The body segments in stance phase are labelled by red circle. (b) The illustration of the force-velocity relationship. (Left) The vector of body velocity ($\xi$) and GRF $f$ on the body segment in contact with environments (red cube). (Right) The decomposition of body velocity and GRF in the direction of body orientation.
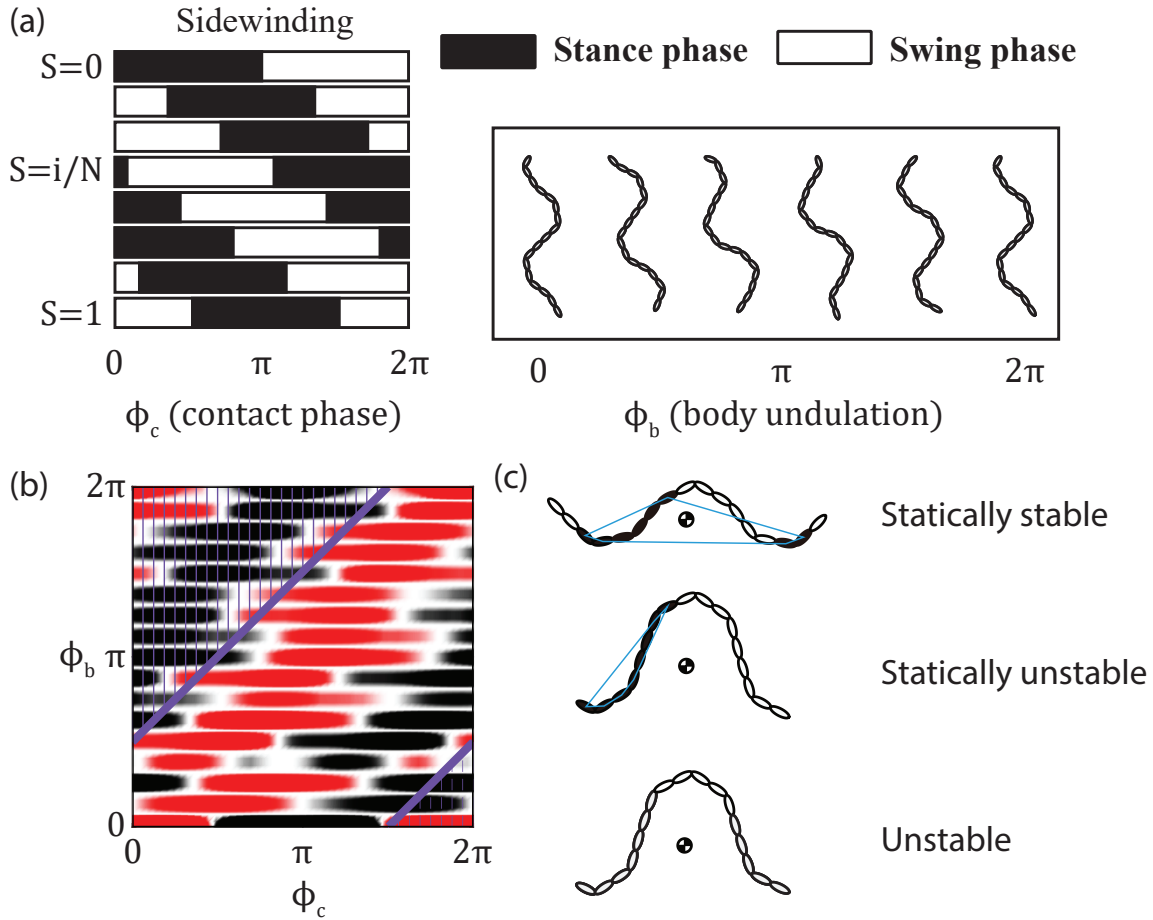
Figure S4: **An example of gait design for sidewinding robot using Hildebrand gait principles.** From the parameter space (a. left), we select the duty factor $D$ and lateral phase lag $\Phi_{lat}$. We prescribe the contact by its phase $\phi_c$ (a. right), and the lateral body undulation by its phase $\phi_b$ (a.3). (b) The height functions to design gait. The gait path (the purple curve) is designed to maximize the volume enclosed in the lower right corner (in solid shadow) minus the volume enclosed in the upper left corner (in dashed shadow). We illustrated the typical configurations that the robot is statically stable, statically unstable, and unstable.
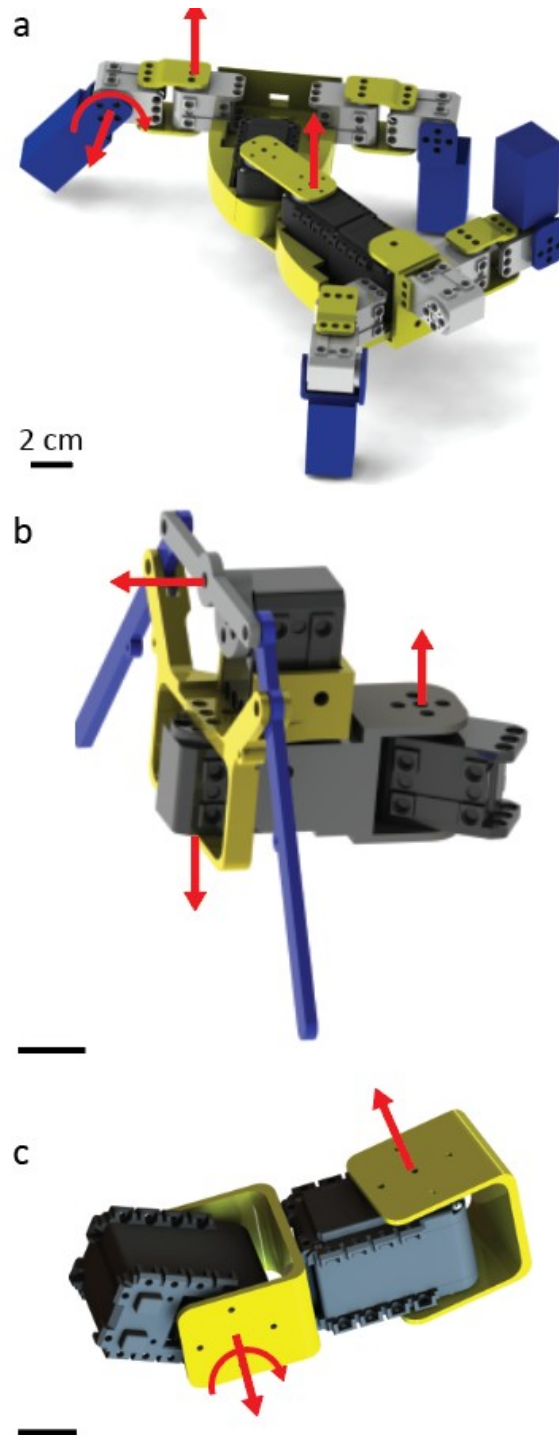
Figure S5: **Joint rotation angles of the robots.** Red arrows show the rotation axis of the joints. **(a)** Quadruped robot **(b)** A segment of the hexapod (includes 3 segments) and myriapod (includes 8 segments) robots. (c) A segment of the sidewinder robot (includes 7 segments). All scale bars are equal to 2 cm.